Biosensors and Bioelectronics 87 (2017) 122–128

Contents lists available at ScienceDirect

Biosensors and Bioelectronics

journal homepage: www.elsevier.com/locate/bios

A universal multicolor immunosensor for semiquantitative visual detection of biomarkers with the naked eyes

Xiaoming Ma [a,b], Yue Lin [a,b], Longhua Guo [a,b,*], Bin Qiu [a,b], Guonan Chen [a,b], Huang-hao Yang [a,b], Zhenyu Lin [a,b,*]

[a] State Key Laboratory of Photocatalysis on Energy and Environment, College of Chemistry, Fuzhou University, Fuzhou, Fujian, 350116 China
[b] MOE Key Laboratory of Analysis and Detection for Food Safety, Fujian Provincial Key Laboratory of Analysis and Detection Technology for Food Safety, Institute of Nanomedicine and Nanobiosensing, College of Chemistry, Fuzhou University, Fuzhou, Fujian, 350116 China

ARTICLE INFO

Article history:
Received 27 May 2016
Received in revised form
7 August 2016
Accepted 8 August 2016
Available online 8 August 2016

Keywords:
Immunoassay
Gold nanorods
Colorimetric detection
Carcinoembryonic antigen
ELISA

ABSTRACT

3, 3′, 5, 5′-tetramethylbenzidine (TMB) has been widely used as a chromogenic substrate for colorimetric immunoassays. Normally, the colorless TMB is oxidized into yellow TMB^{2+} (in acidic solution) to indicate the presence of the target molecules. However, this kind of monochromic intensity changes seriously confine the accuracy of visual inspection. Herein, we demonstrate for the first time that TMB^{2+} can quantitatively and efficiently etch gold nanorods (AuNRs). The addition of AuNRs into a solution containing different amount of TMB^{2+} generates vivid color responses as colorful as a rainbow, and the etching process can be finished within 90 s. As a result, the exact concentration of TMB^{2+} can be easily distinguished with the naked eyes by the corresponding solution color. Based on this finding, we incorporate AuNRs into the well-developed, commercially available horseradish peroxidase (HRP)-TMB immunoassay system, so that it can be utilized for semiquantitative detection of a broad range of disease biomarkers with the naked eyes (termed 'NEQ-IA'). Carcinoembryonic antigen (CEA) and Prostate specific antigen (PSA) had been chosen as example targets to test the feasibility of the proposed biosensor. The results showed good accordance with the conventional methods. Because no sophisticated apparatus but human eyes are used as the readout, the proposed NEQ-IA could be a good supplementary to current state-of-the-art immunoassay methods for those applications that require the use of portable and affordable devices, for example, for the detection of disease biomarkers at home and in the field.

1. Introduction

Immunoassays have been widely used in the hospital for the detection of all kinds of disease biomarkers. It shows high specificity via antibody-antigen recognition and high sensitivity via enzyme-triggered signal amplification (Brennan et al., 2010; Ito et al., 2014). Normally, immunoassay is conducted in the hospital with an automatic microplate reader. It is worth to note that the expensive and bulky microplate reader seriously confines the utility of conventional immunoassay approaches for point-of-care (POC) diagnostics and in-home personal healthcare (Qu et al., 2011; Yan et al., 2013). In order to meet these challenges, an accessible and affordable detection device should be developed to replace the sophisticated readout (Tram et al., 2014; Zhu et al., 2015). In this regard, naked-eye inspection could be a good choice because it does not involve the use of any analytical devices but human eyes for the detection (Liu et al., 2013; Xia et al., 2010; Zhou et al., 2008, 2010).

Although colorimetric immunoassay kits that enable naked-eye inspection are already commercially available, most of them can be only used for qualitative detection of disease biomarkers due to the limited colors displayed in response with different concentrations of targets. For example, the widely used horseradish peroxidase (HRP)-3, 3′, 5, 5′-tetramethylbenzidine (TMB) immunoassay system shows monochromic (yellow) intensity change in response to the variations of target concentrations (John Goka and Farthing, 1987). Recently, Stevens and coworkers (de la Rica and Stevens, 2012, 2013) reported a plasmonic immunoassay approach for sensitive determination of disease biomarkers that generated dual color response (red and blue) in the presence and absence of the analytes. It was reported that this kind of dual color response was easier to be distinguished by human eyes than the conventional single color immunoassay. Even though, color

* Corresponding authors at: State Key Laboratory of Photocatalysis on Energy and Environment, College of Chemistry, Fuzhou University, Fuzhou, Fujian 350116, China.
E-mail addresses: guolh@fzu.edu.cn (L. Guo), zylin@fzu.edu.cn (Z. Lin).

http://dx.doi.org/10.1016/j.bios.2016.08.021
0956-5663/

transformation between red and blue was still not accurate enough for quantifying the concentration of the target molecules without the aid of a spectrometer (de la Rica and Stevens, 2012).

Experts estimated that human eyes can distinguish as many as 10 million of different colors (Wyszecki, 2006). Therefore, we believe that the accuracy of visual inspection can be greatly improved as long as plenty of colors are presented in the presence of different amount of target molecules. In order to develop such a multicolor immunoassay, the searching of an appropriate chromogenic substrate that shows vivid color variations upon the addition of targets is important. Noble metal nanostructures could be potential candidates because the solution color of noble metal nanoparticles is highly dependent on their size, shape and composition (Anker et al., 2008; Meinzer et al., 2014). In fact, in recent years, noble metal nanostructures have been widely explored for the construction of colorimetric sensors (Elghanian et al., 1997; Guo et al., 2015, 2013; Swierczewska et al., 2012; Zhou et al., 2015). Among diverse metal nanostructures, Au nanorods (AuNRs) could be an idea chromogenic substrate for multicolor display because the longitudinal plasmon bands of AuNRs are easily to be tuned by adjusting their aspect ratios (Huang et al., 2006; Kabashin et al., 2009). Various aspect ratios of AuNRs display a range of different color as colorful as a rainbow (Tsung et al., 2006; Vigderman et al., 2012; Ni et al., 2008). These vivid colors can be easily distinguished by naked eyes. Most recently, we demonstrated that AuNRs were ideal colorful chromogenic substrates for colorimetric immunoassays, and the proposed approach was utilized for semiquantitative detection of nucleic acids, proteins and small molecules with the naked eye (Ma et al., 2016). However, this method required labeling the antibody with catalase. Thus it cannot well accommodate conventional immunoassay platforms (Xianyu et al., 2014).

In this work, we disclose for the first time that the product (TMB^{2+}) of HRP catalyzed oxidation of TMB can quantitatively etch AuNRs. Based on this finding, we develop a novel immunoassay scheme that utilizes HRP as the enzyme label and TMB-AuNRs mixture as the chromogenic substrate. Carcinoembryonic antigen (CEA) and Prostate specific antigen (PSA) were widely investigated as disease biomarkers during the cancer diagnosis, therefore, we choose them as model targets to verify the performance of our scheme (Choi et al., 2013; Gao et al., 2015; Han et al., 2016; Zhai et al., 2015, 2016). By using this novel immunoassay scheme, the solutions display vivid colors in response to concentration variations of disease biomarker so that visual quantification of the analyte is achieved. We define this novel approach as naked-eye semiquantitative immunoassay (NEQ-IA) in order to distinguish it from those conventional immunoassay methods that detected with sophisticated readouts. Since HRP has been widely used as enzyme labels in commercial available immunoassay kits, the proposed NEQ-IA is easily to accommodate conventional immunoassays for the detection of a large number of disease biomarkers.

2. Experimental section

2.1. Reagents

CEA ELISA test kits and control solutions were purchased from Biocell Biotechnol. Co., Ltd. (Zhengzhou, China). The ELISA kit comprised a microtiter plate coated with anti-CEA (monoclonal), anti-CEA-HRP conjugate (polyclonal), urea peroxide (0.05%), TMB (1.25 g/mL), 2 M sulfuric acid, a surfactant wash buffer (WB), and a series of CEA standards. Human PSA-total ELISA Kit was obtained from Sigma Aldrich Chemical Co. (USA). TMB Substrate A and B were obtained from Aladdin Chemistry Co., Ltd (Shanghai, China). Lyophilized Horseradish peroxidase (HRP, EC 1.11.1.7, $A > 300$ U/mg) was purchased from Sangon Biotech Co. Ltd. (Shanghai, China). Gold (III) chloride trihydrate (99.9%) ($HAuCl_4 \cdot 4H_2O$), cetyltrimethyl ammonium bromide (CTAB), sodium borohydride ($NaBH_4$), silver nitrate ($AgNO_3^-$) and ascorbic acid were purchased from Sinopharm Chem. Re. Co., Ltd. (Shanghai, China). All other chemicals were of extra pure analytical grade and used without further purification. All solutions were prepared with deionized water obtained from a Milli-Q water purifying system (≥ 18 MΩ, Milli-Q, Millipore). Clinical serum samples were made available by Fujian Provincial Hospital, China. The serum samples had already been processed as required and were therefore ready for analysis.

2.2. Instruments

Extinction spectra of AuNRs solutions were measured using a Microplate Spectrophotometer (Multiskan GO, Thermo Scientific, USA) at room temperature. Transmission electron microscopy (TEM, Tecnai G2 F20 S-TWIN, FEI, USA) was used to study the different oxidation stage of the AuNRs. The photographs of the reaction wells were taken with a Canon digital camera.

2.3. Synthesis of the starting gold nanorods

AuNRs were synthesized by a silver ion-assisted seed mediated method (Nikoobakht et al., 2003; Ye et al., 2013). In brief, the seed solution was prepared by adding a freshly prepared, ice-cold $NaBH_4$ solution (0.01 M, 0.6 mL) into a solution containing $HAuCl_4$ (0.005 M, 5 mL) and CTAB (0.2 M, 5 mL) in a 15 mL glass tube under vigorous stirring (1200 rpm). After vigorous stirring for 2 min, the color of the seed solution turned from yellow to brownish yellow. Then the stirring was turned off and the seed solution was kept at room temperature for at least 30 min before use. To prepare the growth solution, ascorbic acid (5.5 mL, 0.1 M) was added to a well-mixed solution containing $HAuCl_4$ (5 mL, 0.01 M), $AgNO_3$ (0.60 mL, 0.01 M), and CTAB (50 mL, 0.2 M). The mixture solution was diluted to 100 mL with deionized water. Finally, 200 μL of the seed solution was injected into the growth solution. The resultant mixture was vigorously stirred for 30 s and then left undisturbed at 30 °C for 24 h. The as-synthesized AuNRs was centrifuged at 11,000 rpm for 15 min followed by removal of the supernatant. Then the precipitate was redispersed into 0.06 M CTAB solution with the same volume. The same separation procedures were repeated twice to obtain a final solution containing AuNRs and 0.06 M CTAB. This solution was utilized as chromogenic substrate for color display in the subsequent experiments. The concentration of this AuNRs stock solution was ~0.24 nM, as calculated according to an extinction coefficient of AuNRs at 744 nm of $4.13 \pm 0.5 \times 10^9\ M^{-1}\ cm^{-1}$(Orendorff and Murphy, 2006).

2.4. TMB^{2+} titration experiments

The TMB^{2+} stock solution was synthesized via the ultraviolet radiation of TMB. Briefly, 2 mL TMB solution was irradiated under 337 nm laser irradiation for 10 min and then 1 M HCl solution (1 mL) was added. The concentration of TMB^{2+} in the final solution was 167 μM, calculated by the extinction coefficient of the diimine, $\varepsilon = 5.9 \times 10^4\ M^{-1}\ cm^{-1}$ (Josephy et al., 1982). Different concentration of TMB^{2+} solutions were prepared by dilution of the TMB^{2+} stock solution with distilled water. 100 μL AuNRs solution (concentration of Au[0] was ~0.69 ± 0.01 mM as measured by ICP-MS) was added into each prepared TMB^{2+} solution and the mixture solutions were allowed to incubate for 2 min before spectral measurements.

2.5. Construction of the CEA standard reference card

The CEA standard reference card was prepare by a series of CEA standard solutions, the concentrations were 0, 2.5, 5, 7.5, 10, 12.5, 15, 17.5, 20, 22.5, 25, 27.5, 30, 32.5, 35, 37.5, 40, 42.5, 45, 47.5, 50, 52.5, 55, 60 ng/mL. The procedures were followed by the manual of the commercial ELISA kit. In brief, 50 μL CEA standards (0–60 ng/mL) were added into the appropriate wells which containing immobilized mouse monoclonal antibody against CEA. Then Anti-CEA-HRP conjugate (50 μL) was added into each well. Covered the plate and incubated for 1 h at 37 °C. After incubation, the wells were aspirated and washed four times with a surfactant washing buffer. Anti-CEA-HRP conjugate (100 μL) was added to each well and incubated for 1 h at 37 °C. Following another series of wash steps with washing buffer, substrate solution (TMB/H_2O_2, 100 μL) was added, and the reaction was left to proceed for 20 min at room temperature. For the yellow diimine oxidation product (TMB^{2+}), analysis took place after the addition of 1 M HCl solutions (50 μL). Then 100 μL AuNRs were added into the solution with gently mixed for 90 s. The colors of the constructed standard reference card were recorded by the camera.

3. Results and discussion

3.1. Mechanism of the proposed biosensor

The experimental setup of the proposed NEQ-IA immunosensor is similar to the conventional colorimetric ELISA with the only difference in the color-display step: in the conventional ELISA an acidic solution is added to display a color, whereas in our proposed method a mixture solution consisting of acid and AuNRs is added to display various colors (Scheme 1). AuNRs can react with TMB^{2+} to produce TMB°, and meanwhile, Au was oxidized into Au(I). In the presence of CTAB, this oxidation process selectively takes place at the ends of AuNRs, thus the AuNRs are shortened while keeping the diameter nearly unaltered (Tsung et al., 2006; Ni et al., 2008). As a result, the aspect ratios of AuNRs gradually decrease with the increase of TMB^{2+}, and the solution displays a colorful transition as shown in Scheme 1 (the color pictures located at the lower right corner). When AuNRs are oxidized to an aspect ratio of ~1, the solution color turned to red, which is similar to the color of spherical Au nanoparticles. Further increase the amount of TMB^{2+} would gradually turn the solution to colorless, which indicates that all Au nanoparticles have been oxidized into Au(I). The colorless solution would gradually turn into yellow if additional TMB^{2+} is added.

3.2. Mechanism of TMB^{2+} induced oxidation of AuNRs

It is worth noting that H_2O_2 can oxidize AuNRs in the presence of Br^- under acid condition at high temperature (Ni et al., 2008). However, under the reaction conditions of our experiments, neither H_2O_2 nor HRP showed obvious oxidizing ability to AuNRs. On the contrary, TMB^{2+} can oxidize AuNRs rapidly, resulting in a blue shift of longitudinal plasmon band (LPB) at room temperature (see Fig. 1 and Fig. S1). In order to confirm that the selective shortening of AuNRs was caused by TMB^{2+}, TMB^{2+} titration experiments were conducted (see Fig. 2).

Fig. 2A(a) shows the corresponding UV–vis spectra of the titration. The starting AuNRs exhibited two extinction peaks in the visible region at ~744 nm and ~511 nm, corresponding to the longitudinal plasmon band (LPB) and transverse plasmon band (TPB) of AuNRs, respectively. After the addition of TMB^{2+}, the extinction spectra of AuNRs appeared significant LPB blue shifts, and the amount of peak shifts were closely related to the concentration of TMB^{2+}. As it can be seen from Fig. 2A(b), good linearity was observed between the LPB peak locations and the added amount of TMB^{2+}. The good linearity between TMB^{2+} and the LSPR shifts suggested that TMB^{2+} was quantitatively reacted with AuNRs. It should be noted that the kinetics of TMB^{2+} induced shortening of AuNRs was a quick process within 90 s. Upon further addition of TMB^{2+}, the LPB disappeared and only TPB was recorded, indicating the transformation of nanorods into nanospheres. Instead of peak shift, significant peak intensity decreases of TPB were observed when increasing the concentration of TMB^{2+}. In this case, the intensities of the TPB peaks were decreased exponentially with the concentration of TMB^{2+} (see Fig. 2A(c)). Au nanospheres were etched up eventually, as indicated by the disappearance of the extinction peak and the solution was colorless in this case. Normally, Au can be oxidized into Au(I) or Au(III) by different oxidizers. The colorless solution obtained in our experiments suggests that the oxidation product of Au should be Au(I) (in the form of $AuBr_2^-$ in the presence of CTAB) because $AuBr_2^-$ is colorless while Au(III) ($AuBr_4^-$) is yellow. After the solution turned into colorless, further increase the concentration of TMB^{2+} generates a new absorption peak at ~450 nm, which corresponds to the absorption of TMB^{2+}. This indicates that the excess TMB^{2+} cannot oxidize Au(I) into Au(III). The additional TMB^{2+} is still in its original form. The peak intensity at ~450 nm shows good linearity with the added amount of concentration of TMB^{2+} (Fig. 2A(d)).

This etching process was further confirmed by transmission electron microscopy (TEM) (Fig. 3). Statistical analysis from TEM images shows that the length of AuNRs is ~58 nm, and the

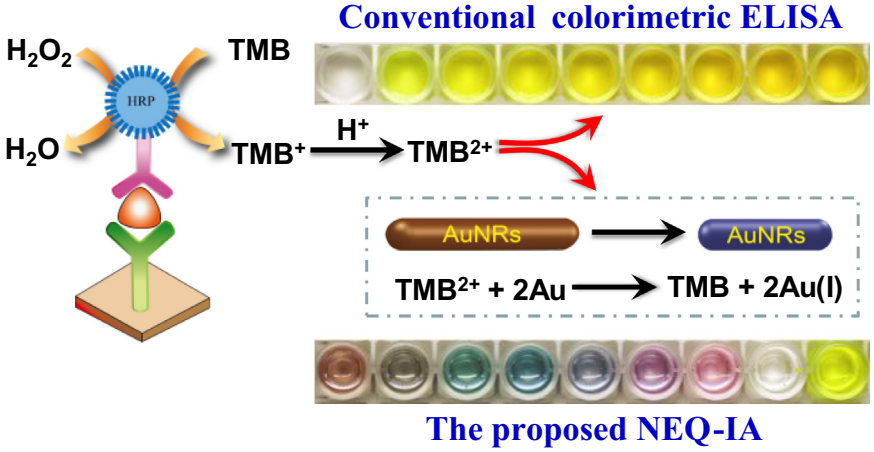

Scheme 1. Comparison of the conventional colorimetric ELISA and NEQ-IA ELISA.

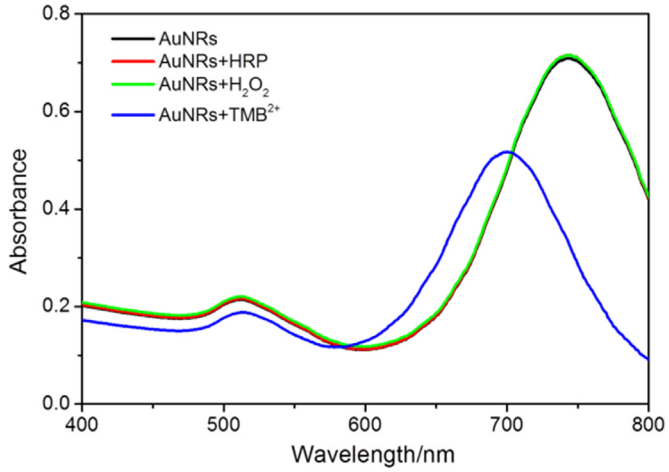

Fig. 1. Absorbance spectra measurement of different reagents effect on the AuNRs oxidation. (line in black) the as-synthesis AuNRs; (line in red) the as-synthesis AuNRs mixed with 150 μL 0.3 U/L HRP; (line in green) the as-synthesis AuNRs mixed with 150 μL 2 mM H_2O_2 and (line in blue) the as-synthesis AuNRs mixed with 150 μL 21.8 μM TMB^{2+}. The volume of AuNRs is 100 μL and the final volumes of the above solutions are 250 μL. (For interpretation of the references to color in this figure legend, the reader is referred to the web version of this article.)

average diameter is ~20 nm before etching. After the addition of TMB^{2+}, the length of AuNRs was gradually reduced while the diameter stays almost unaltered. The Au nanoparticles are almost quasi-spherical for a solution which displays red color (the last picture of Fig. 3). These results strongly indicated that the oxidation of AuNRs was closely related to the concentration of TMB^{2+} presented in the solution.

3.3. Visual quantification of biomarkers

Next, we demonstrated the feasibility of the proposed NEQ-IA for visual inspection of disease biomarkers in human serum. The detection of tumor marker, CEA, was selected as demonstration. All the assay procedures were followed by the instructions of the kit except for the addition of an AuNRs solution to the final solution and then incubated for 90 s. The amount of AuNRs was related to the color of solution as discussed above, we choose 100 μL 0.24 nM AuNRs to a total volume 250 μL as the optimized concentration added because it exhibits a vivid color display than the others (See Fig. S2). As we know, in the conventional ELISA procedure, the concentration of TMB^{2+} is corresponding with the contents of analytical target, while the amounts of TMB^{2+} can quantitative react with AuNRs through our proposed method.

Therefore, we constructed a standard reference card by react with a series of standard solutions. In the conventional ELISA, the solutions color turn into yellow in the presence of analytical targets (see Fig. S3). By the means of our proposed method, a series of colorful solutions would turn up after the addition of AuNRs. Therefore, the concentration of the unknown sample can be achieved by the following visual quantitative procedure: firstly, the color of the sample solution was compared with the standard reference card (Fig. 4A, Fig. S4A). If the color of a sample was close to the color of one of the standard color solutions shown in Fig. 4A, then the concentration of the standard color solution was designated for the sample; if the color of the sample was in between the colors of two standard solutions, then the average value of the two standard solutions was designated as the concentration of the sample. The limit of detection (LOD) for CEA was ~2.5 ng/mL, which was similar to the commercial available ELISA Kit (2.5 ng/mL as indicated in the specification of the Kit). It is worth to note that the LOD of our method was obtained based on visual detection, while the LOD of the commercial ELISA Kit was

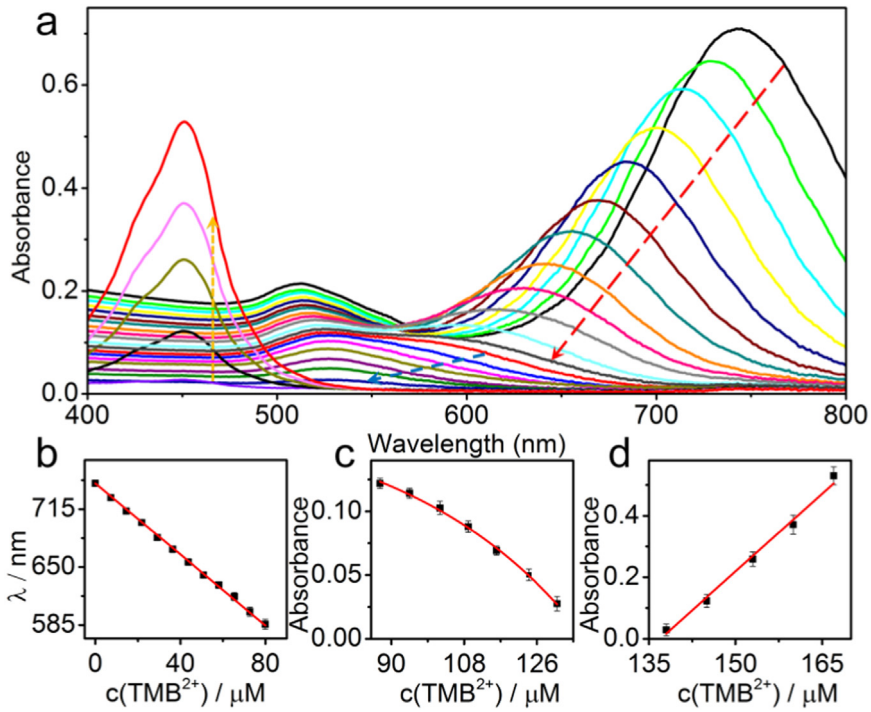

Fig. 2. (A) TMB^{2+} titration experiments. (a) UV spectra of 100 μL of AuNRs (~0.24 nM) reacted with 150 μL TMB^{2+} with different concentrations: (spectra cover by the red dashed arrow) 0, 7.27, 14.5, 21.8, 29.1, 36.3, 43.6, 50.9, 58.1, 65.4, 72.7, 79.9 μM, respectively; (spectra cover by the blue dashed arrow) 87.2, 94.5, 102, 109, 116, 124, 131 μM, respectively; (spectra cover by the yellow dashed arrow) 138, 145, 153, 160, 167 μM, respectively; (b) LPB shifts of AuNRs as a function of the TMB^{2+} concentration in the range of 0–79.9 μM (spectra cover by the red dashed arrow); (c) Peak intensity changes at 526 nm as a function of the TMB^{2+} concentration in the range of 87.2–131 μM (spectra cover by the blue dashed arrow); (d) Peak intensity changes at 450 nm as a function of the TMB^{2+} concentration in the range of 138–167 μM (spectra cover by the yellow dashed arrow). (For interpretation of the references to color in this figure legend, the reader is referred to the web version of this article.)

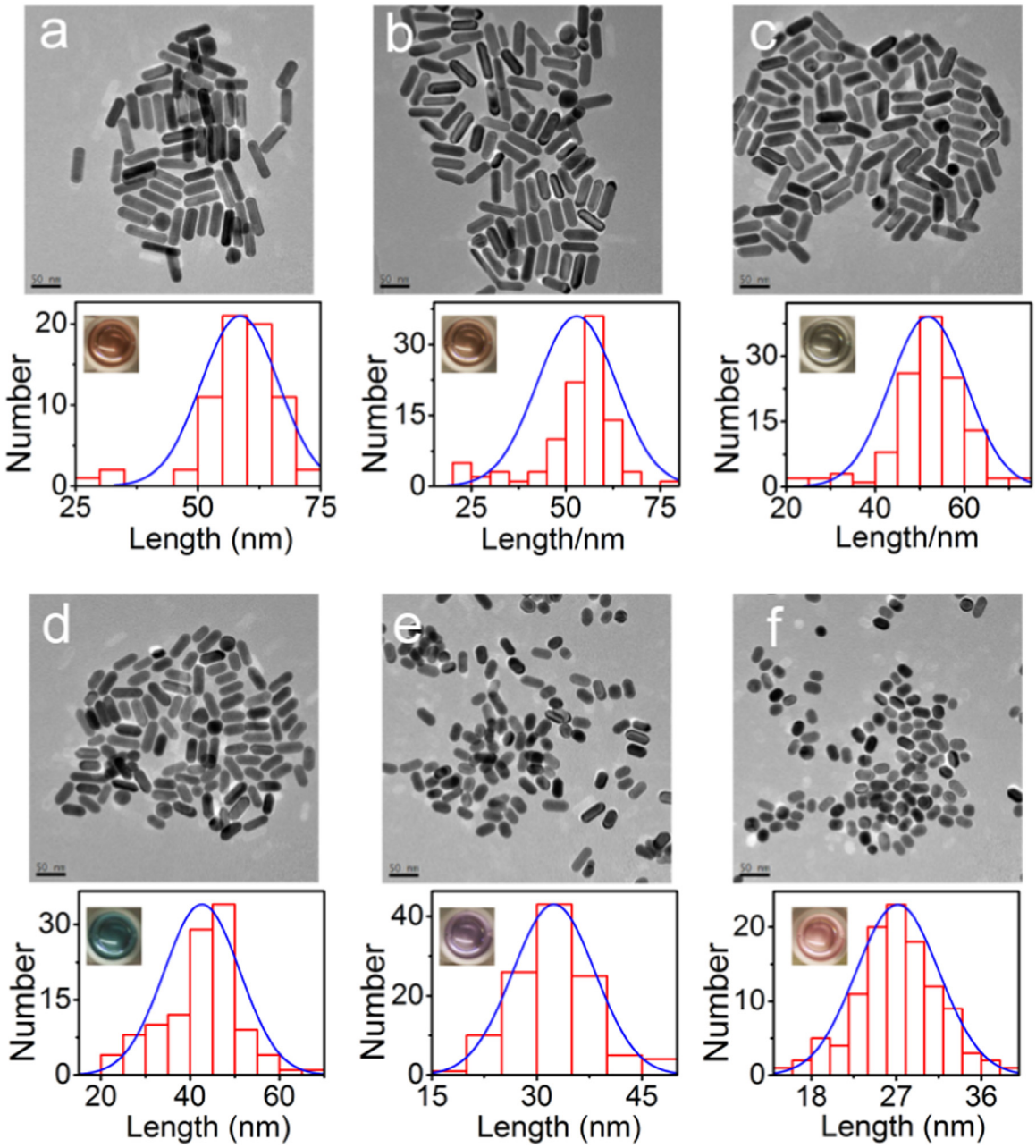

Fig. 3. TEM images and corresponding statistical analysis of the AuNRs before and after etching with different concentrations of TMB^{2+}. The insets show the photos of the corresponding solutions. Scale bars =50 nm.

calculated based the signal from a microplate.

Fig. 5A and Fig. S4B shows the quantification results of CEA the serum samples by the full color immunosensor proposed in this work, the commercial ELISA kits, and the chemiluminescence immunoassay (CLIA) conducted in the hospital. Noting that CLIA utilized a sophisticated automated chemiluminescent immunoassay analyzer for quantification; the commercial ELISA used an expensive microplate reader for CEA determination, and only the proposed NEQ-IA method used visual inspection for CEA quantification. Good consistency was observed among the three methods. These results strongly indicate the potential applicability of the proposed NEQ-IA strategy for clinical diagnosis. Moreover, our proposed NEQ-IA strategy shows good stability as shown in the Fig. S6. In order to verify the wide applicability of our proposed method, visual detection of the other biomarker PSA was also detection by our method. The PSA standard reference card was constructed (see Fig. 4B, Fig. S5A), and the results of actual samples were shown in the Fig. 5B and Fig. S5B. The limit of detection (LOD) for PSA was ~75 pg/mL, which was variable for the early detection of prostate cancer.

4. Conclusions

In summary, this work disclosed that the product (TMB^{2+}) of the enzymatic reaction of conventional HRP-TMB system can quantitatively etch AuNRs to generate rapidly vivid color responses. Based on this finding, we demonstrated a proof-of-concept NEQ-IA method that can be used for visual quantification of a broad range of the analytes with the naked eyes. Similar to pH test, the concentration of analytes can be easily distinguished by comparing the solution color with a standard reference card (a

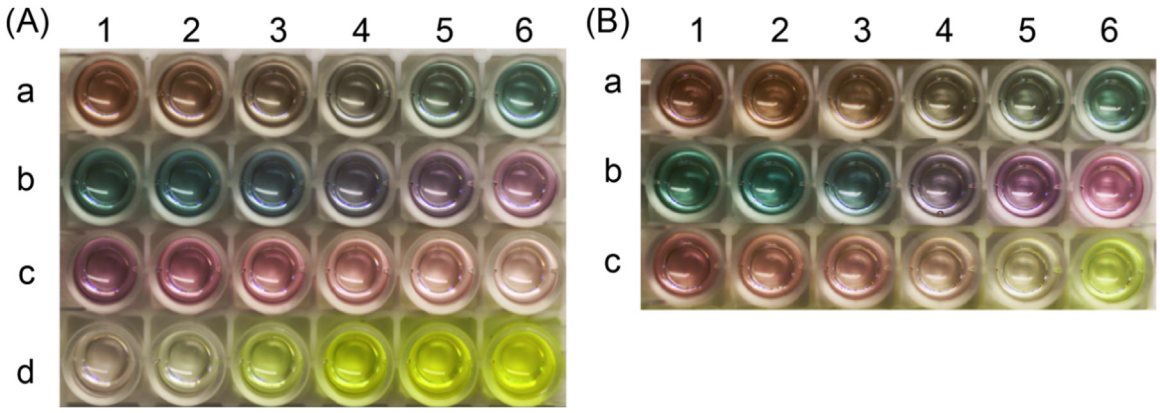

Fig. 4. Photos of different amount of CEA (A) and PSA (B) standard solutions after the addition of 100 μL AuNRs solution. The concentrations of CEA are as follows: a1～a6: 0, 2.5, 5, 7.5, 10, 12.5 ng/mL; b1～b6: 15, 17.5, 20, 22.5, 25, 27.5 ng/mL; c1～c6: 30, 32.5, 35, 37.5, 40, 42.5 ng/mL; d1～d6: 45, 47.5, 50, 52.5, 55, 60 ng/mL. The concentrations of PSA are as follows: a1～a6: 0, 75, 150, 225, 300, 375 pg/mL; b1～b6: 450, 525, 600, 675, 750, 825 pg/mL; c1～c6: 900, 975, 1050, 1125, 1200, 1275 pg/mL.

(A)

ng/ml	CLIA	Conventional ELISA	This Method
	7.8±0.31	7.2±0.82	7.5
	21.1±0.82	19.7±2.68	20
	39.1±3.86	35.1±3.26	36.25
	14.6±0.90	13.9±1.49	13.75
	45.2±2.65	43.9±2.57	43.75
	48.1±3.15	53.2±3.09	50

(B)

pg/ml	CLIA	Conventional ELISA	This Method
	830±8.7	837±7.2	825
	781±4.83	790±6.63	787.5
	453±2.91	448±3.19	450
	220±3.71	224±3.42	225
	335±3.64	340±4.87	337.5
	78±3.6	79±4.1	75

Fig. 5. Visual quantification of CEA (A) and PSA (B) by the proposed NEQ-IA ELISA.

piece of colored paper) with the naked eyes. Comparing with the conventional ELISA, the proposed NEQ-IA did not involve the use of the costly and bulky readout (e.g. the automatic microplate reader).

Acknowledgment

This project was partly financially supported by National Natural Science Foundation of China (21575027, 21277025 and 21275017) and the Natural Science Foundation of Fujian Province for Distinguished Young Scholar (2014J06005). We also thank Dr. X. Li of the First Affiliated Hospital of Fujian Medical University for providing the serum samples and the CLIA assay results of CEA and PSA.

Appendix A. Supplementary material

Supplementary data associated with this article can be found in the online version at http://dx.doi.org/10.1016/j.bios.2016.08.021.

References

Anker, J.N., Hall, W.P., Lyandres, O., Shah, N.C., Zhao, J., Van Duyne, R.P., 2008. Nat. Mater. 7 (6), 442–453.
Brennan, D.J., O'Connor, D.P., Rexhepaj, E., Ponten, F., Gallagher, W.M., 2010. Nat. Rev. Cancer 10 (9), 605–617.
Choi, J.H., Kim, H.S., Choi, J.-W., Hong, J.W., Kim, Y.-K., Oh, B.-K., 2013. Biosens. Bioelectron. 49, 415–419.
Elghanian, R., Storhoff, J.J., Mucic, R.C., Letsinger, R.L., Mirkin, C.A., 1997. Science 277 (5329), 1078–1081.
Gao, J., Guo, Z., Su, F., Gao, L., Pang, X., Cao, W., Du, B., Wei, Q., 2015. Biosens. Bioelectron. 63, 465–471.
Guo, L., Xu, Y., Ferhan, A.R., Chen, G., Kim, D.H., 2013. J. Am. Chem. Soc. 135 (33), 12338–12345.
Guo, L., Jackman, J.A., Yang, H.-H., Chen, P., Cho, N.-J., Kim, D.-H., 2015. Nano Today 10 (2), 213–239.
Han, J., Jiang, L., Li, F., Wang, P., Liu, Q., Dong, Y., Li, Y., Wei, Q., 2016. Biosens. Bioelectron. 77, 1104–1111.
Huang, X., El-Sayed, I.H., Qian, W., El-Sayed, M.A., 2006. J. Am. Chem. Soc. 128 (6), 2115–2120.
Ito, Y., Hashimoto, M., Hirota, K., Ohkura, N., Morikawa, H., Nishikawa, H., Tanaka, A., Furu, M., Ito, H., Fujii, T., 2014. Science 346 (6207), 363–368.
John Goka, A., Farthing, M.J., 1987. J. Immunoass. 8 (1), 29–41.
Josephy, P.D., Eling, T., Mason, R.P., 1982. J. Biol. Chem. 257 (7), 3669–3675.
Kabashin, A., Evans, P., Pastkovsky, S., Hendren, W., Wurtz, G., Atkinson, R., Pollard, R., Podolskiy, V., Zayats, A., 2009. Nat. Mater. 8 (11), 867–871.
de la Rica, R., Stevens, M.M., 2012. Nat. Nanotechnol. 7 (12), 821–824.
de la Rica, R., Stevens, M.M., 2013. Nat. Protoc. 8 (9), 1759–1764.
Liu, D., Wang, Z., Jin, A., Huang, X., Sun, X., Wang, F., Yan, Q., Ge, S., Xia, N., Niu, G., Liu, G., Walker, A.R.H., Chen, X., 2013. Angew. Chem. Int. Ed. 52 (52), 14065–14069.
Ma, X., Chen, Z., Kannan, P., Lin, Z., Qiu, B., Guo, L., 2016. Anal. Chem. 88 (6), 3227–3234.
Meinzer, N., Barnes, W.L., Hooper, I.R., 2014. Nat. Photonics 8 (12), 889–898.
Ni, Weihai, Kou, Xiaoshan, Yang, Zhi, Wang, J., 2008. ACS Nano 2 (4), 677–686.
Nikoobakht, B., El-Sayed, M.A., 2003. Chem. Mater. 15 (10), 1957–1962.
Orendorff, C.J., Murphy, C.J., 2006. J. Phys. Chem. B 110 (9), 3990–3994.
Qu, W., Liu, Y., Liu, D., Wang, Z., Jiang, X., 2011. Angew. Chem. Int. Ed. 50 (15), 3442–3445.
Swierczewska, M., Liu, G., Lee, S., Chen, X., 2012. Chem. Soc. Rev. 41 (7), 2641–2655.
Tram, K., Kanda, P., Salena, B.J., Huan, S.Y., Li, Y.F., 2014. Angew. Chem. Int. Ed. 53 (47), 12799–12802.
Tsung, C.K., Kou, X., Shi, Q., Zhang, J., Yeung, M.H., Wang, J., Stucky, G.D., 2006. J. Am. Chem. Soc. 128 (16), 5352–5353.
Vigderman, L., Khanal, B.P., Zubarev, E.R., 2012. Adv. Mater. 24 (36), 4811–4841.

Wyszecki, G., 2006. Color. World Book Inc, Chicago.
Xia, F., Zuo, X., Yang, R., Xiao, Y., Kang, D., Vallée-Bélisle, A., Gong, X., Yuen, J.D., Hsu, B.B., Heeger, A.J., 2010. Proc. Natl. Acad. Sci. USA 107 (24), 10837–10841.
Xianyu, Y., Wang, Z., Jiang, X., 2014. ACS Nano 8 (12), 12741–12747.
Yan, L., Zhu, Z., Zou, Y., Huang, Y., Liu, D., Jia, S., Xu, D., Wu, M., Zhou, Y., Zhou, S., 2013. J. Am. Chem. Soc. 135 (10), 3748–3751.
Ye, X., Zheng, C., Chen, J., Gao, Y., Murray, C.B., 2013. Nano Lett. 13 (2), 765–771.
Zhai, Q., Zhang, X., Xia, Y., Li, J., Wang, E., 2016. Analyst . http://dx.doi.org/10.1039/C6AN00675B.
Zhai, Q., Zhang, X., Han, Y., Zhai, J., Li, J., Wang, E., 2015. Anal. Chem. 88 (1), 945–951.
Zhou, W., Gao, X., Liu, D., Chen, X., 2015. Chem. Rev. 115 (19), 10575–10636.
Zhou, Y., Wang, S., Zhang, K., Jiang, X., 2008. Angew. Chem. Int. Ed. 47 (39), 7454–7456.
Zhu, Z., Wu, C., Liu, H., Zou, Y., Zhang, X., Kang, H., Yang, C.J., Tan, W., 2010. Angew. Chem. Int. Ed. 49 (6), 1052–1056.
Zhu, Z., Guan, Z.C., Liu, D., Jia, S.S., Li, J.X., Lei, Z.C., Lin, S.C., Ji, T.H., Tian, Z.Q., Yang, C. Y.J., 2015. Angew. Chem. Int. Ed. 54 (36), 10448–10453.